processes

MDPI

Article

Rock-Physics-Constrained Intelligent Porosity Prediction for Fracture–Vuggy Carbonate Reservoirs: A Case Study from the XX Well Block, Tarim Oilfield

Haitao Zhao [1,2,3,4], Xingliang Deng [1,2,3,*], Yufan Lei [5], Zhengyang Li [1,2,3,4], Yuan Ma [1,2,3,4] and Ziran Jiang [6]

[1] PetroChina Tarim Oilfield Company, Korla 841000, China; zhaoht-tlm@petrochina.com.cn (H.Z.)
[2] R&D Center for Ultra Deep Complex Oil and Gas Reservoir Exploration and Development Technology, CNPC, Korla 841000, China
[3] Engineering Research Center for Ultra-Deep Complex Reservoir Exploration and Development, Xinjiang Uygur Autonomous Region, Korla 841000, China
[4] Xinjiang Key Laboratory of Ultra-Deep Oil and Gas, Korla 841000, China
[5] College of Energy (College of Modern Shale Gas Industry), Chengdu University of Technology, Chengdu 610059, China
[6] State Key Laboratory of Oil and Gas Reservoir Geology and Exploitation, Chengdu University of Technology, Chengdu 610059, China
* Correspondence: dxl-tlm@petrochina.com.cn

Abstract

Fracture–vuggy carbonate reservoirs exhibit strong heterogeneity, spatial discontinuity, and highly variable porosity, which limit the effectiveness of traditional seismic attributes and conventional inversion. Focusing on the XX well block in the Tarim Basin, this study develops a rock-physics-constrained Physics-Constrained TransUNet method for intelligent porosity prediction. A carbonate-specific rock-physics model is first established, considering mineral composition, pore type, and water saturation, ensuring physical consistency between porosity, elastic parameters, and seismic responses. On this basis, a deep-learning framework integrating U-Net multi-scale feature extraction and Transformer global modeling is constructed. By embedding rock-physics priors, regularization constraints, and log-derived porosity labels, the method forms a unified physics- and data-driven inversion scheme. Applications to multiple deep wells and 3D post-stack seismic data from the FI7 fault zone demonstrate stable training, rapid convergence, and strong capability in capturing nonlinear porosity–seismic relationships. Compared with conventional inversion, the proposed approach significantly improves prediction accuracy in cavern-dominated intervals, fractured zones, and areas with abrupt porosity changes, while maintaining robust lateral continuity. Inter-well sections and target-layer slices further verify its effectiveness in identifying fracture–dissolution–vug composite reservoirs. The method provides a practical and reliable workflow for porosity prediction in ultra-deep carbonate reservoirs, supporting fine reservoir characterization and sweet-spot evaluation.

Keywords: carbonate reservoirs; rock-physics modeling; deep learning; porosity prediction

Check for updates

Academic Editor: Qingbang Meng

Received: 17 December 2025
Revised: 19 January 2026
Accepted: 29 January 2026
Published: 2 February 2026

Copyright: © 2026 by the authors. Licensee MDPI, Basel, Switzerland. This article is an open access article distributed under the terms and conditions of the Creative Commons Attribution (CC BY) license.

1. Introduction

Carbonate reservoirs represent one of the most significant hydrocarbon-bearing systems worldwide [1–4]. They are extensively developed in major basins across the Middle East, North Africa, and China, including the Tarim, Sichuan, and Ordos basins. These reservoirs play a key role in reserve growth and sustained production in unconventional

and deep hydrocarbon exploration [5,6]. In contrast to clastic reservoirs, carbonate reservoirs undergo far more complex formation and alteration processes. Their pore systems are controlled by variations in depositional facies, diagenetic processes, dissolution, and multiple phases of tectonic deformation. As a result, carbonate reservoirs develop diverse and multi-scale pore structures, including fractures, matrix pores, and vugs. In particular, fracture–vuggy carbonate reservoirs, formed by the combined development of structural fractures and dissolution-enlarged voids, display pronounced heterogeneity, discontinuity, and anisotropy [7,8]. Their seismic signatures—often including bead-like strong reflections, chaotic events, and localized energy anomalies—pose substantial challenges for accurately predicting and characterizing key petrophysical parameters such as porosity.

The Tarim Basin represents China's key region for deep to ultra-deep marine carbonate exploration and production [9,10]. The XX well block is located on the western flank of the Tabei Uplift in northern Tarim. It lies within a NE-trending strike-slip fault system between the Halaha–Tang Depression and the Shuntogole Low Uplift. This area is a typical zone where fault-controlled fracture–vuggy carbonate reservoirs are extensively developed. Multi-phase strike–slip faulting coupled with prolonged hydrothermal alteration has generated a composite "fault–dissolution–vug" reservoir system along major faults and associated secondary faults [8]. Reservoirs are typically buried deeper than 7000 m and exhibit highly complex spatial architectures. Drilling and production results show that high-yield wells are concentrated in fault–karst composite zones and in areas with intense fracture and vug development. Reservoir properties such as porosity and permeability can change abruptly over short distances, reflecting pronounced heterogeneity and discontinuity. Moreover, seismic data at such depths often suffer from low signal-to-noise ratios and limited bandwidth. These issues are mainly caused by strong attenuation and pronounced lateral velocity variations. The limited availability of well control and the susceptibility of logs to high-temperature, high-pressure environments and unstable borehole conditions further constrain the spatial continuity and quantitative reliability of conventional seismic inversion and attribute analysis [11]. Consequently, achieving high-accuracy porosity prediction for the fracture–vuggy carbonate reservoirs in the XX well block—under complex structural settings and strong reservoir heterogeneity—has emerged as a critical scientific challenge for deep-target inversion and sweet-spot evaluation in the Tarim Basin.

Over the last two decades, substantial efforts have been devoted both domestically and internationally to improving the identification and prediction of carbonate reservoirs. Early investigations primarily employed seismic attribute analysis and spectral decomposition to delineate vug bodies and fracture-enhanced zones [12,13]. For instance, studies by Wang et al. and Hendry et al. showed that spectral decomposition combined with impedance inversion can reveal dissolution features, yet the vertical resolution remains fundamentally constrained by seismic wavelength, limiting the detection of fine-scale pore structures [14,15]. The introduction of geostatistical inversion and facies-controlled inversion later shifted reservoir prediction from qualitative characterization toward more quantitative modeling. For instance, Li et al. proposed a two-stage facies-controlled inversion workflow, while Liu et al. incorporated structure tensors with coherence attributes to improve impedance inversion in carbonate settings [16,17]. Despite these advances, most existing approaches still rely heavily on statistical correlations among seismic attributes. The underlying rock-physics mechanisms are often underutilized, which limits predictive reliability. The fundamental rock-physics mechanisms that govern carbonate reservoirs are often underutilized, limiting predictive reliability.

In recent years, the rapid development of artificial intelligence, especially deep learning technology, has provided new ideas for seismic inversion and reservoir parameter prediction under complex reservoir conditions [18–21]. Convolutional neural

networks (CNNs) and their encoder–decoder variants such as U-Net have been extensively applied to seismic facies classification, fracture detection, lithology identification, and porosity prediction [22]. However, the intrinsic architectural constraints of CNNs hinder their ability to model the long-range dependencies essential for characterizing fracture–vug systems. Transformer architectures, driven by self-attention mechanisms, excel in complex image recognition by enabling global context modeling and dynamically emphasizing salient features [23]. Transformer architectures have recently gained attention in geophysical applications. They are particularly effective at modeling long-range dependencies through self-attention mechanisms. The hybrid TransUNet architecture integrates U-Net's multi-scale local feature extraction with the Transformer's global contextual awareness. This enables effective detection of diverse "point–patch–band" fracture/vug patterns and offers a promising pathway for porosity prediction and fracture quantification in complex carbonate reservoirs. Qi et al. developed a CNN–BiLSTM–Transformer hybrid model for porosity estimation in carbonate reservoirs [24]. Yan et al. applied a TransUNet architecture integrating Transformer, U-Net, and dual-attention mechanisms to the detection of carbonate and karst cave systems [25]. However, in ultra-deep and structurally complex areas such as the XX well block, the limited quantity of well control severely restricts purely data-driven approaches, increasing the risk of local overfitting and degrading model performance when extrapolating between wells [26–28]. Moreover, without explicit physical constraints, deep models may achieve statistically high accuracy yet still generate porosity distributions inconsistent with known rock-physics relationships or geological trends, compromising interpretability and limiting generalization [29]. Therefore, integrating carbonate-specific rock-physics mechanisms with sparse well-log constraints offers a critical pathway toward improving the reliability and geological realism of porosity prediction [30,31].

Building on these insights, this study focuses on the fracture–vuggy carbonate reservoirs in the XX well block of the Tarim Basin and proposes a porosity prediction method that integrates rock-physics constraints with well-log supervision. The workflow is grounded in a carbonate-specific rock-physics model that defines quantitative links between porosity, lithology, fluid properties, and elastic parameters. These relationships are incorporated as prior constraints into a unified seismic–well-log learning and inversion framework. In addition, high-confidence porosity logs are used as supervision targets to calibrate the network, enabling a synergistic integration of mechanism-driven and data-driven constraints. By jointly leveraging multi-attribute seismic data and rock-physics responses, the method delivers porosity predictions with improved geological realism and lateral continuity, even in settings with limited well control and pronounced reservoir heterogeneity. The case study from the XX well block demonstrates that the proposed hybrid strategy is effective in identifying highly porous fracture–vug zones and evaluating sweet spots. It offers valuable technical support for fine-scale characterization and development planning of deep carbonate reservoirs.

2. Methods

2.1. Rock-Physics Modeling for Carbonate Reservoirs

To compute the elastic modulus of the rock matrix, we assume that the matrix consists of N mineral constituents with volume fractions V_i. The mixture bulk modulus can then be obtained using the classical Voigt–Reuss–Hill (V–R–H) averaging scheme, which takes the mean of the Voigt upper bound and the Reuss lower bound, as given in Equation (1):

$$X_{\mathrm{m}} = \frac{1}{2}\left[\sum_{i=1}^{N} X_i V_i + \frac{1}{\sum\limits_{i=1}^{N} \frac{V_i}{X_i}}\right], \tag{1}$$

where X_{m} and X_i denote the elastic moduli of the rock matrix and the i-th mineral, respectively. X_{m} may refer to either the bulk or shear modulus. If the formation is assumed to consist of only quartz and clay minerals, then, as in Equation (2):

$$\begin{cases} K_{\mathrm{m}} = \left\{\left[CK_{\mathrm{c}} + (1-C)K_{\mathrm{q}}\right] + \frac{1}{C/K_{\mathrm{c}} + (1-C)/K_{\mathrm{q}}}\right\}/2 \\ G_{\mathrm{m}} = \left\{\left[CG_{\mathrm{c}} + (1-C)G_{\mathrm{q}}\right] + \frac{1}{C/G_{\mathrm{c}} + (1-C)/G_{\mathrm{q}}}\right\}/2 \end{cases}. \tag{2}$$

Once the elastic moduli of the rock matrix are determined, pores are incorporated into the matrix using the Kuster–Toksöz (K–T) model. This porosity inclusion process can be written as Equations (3) and (4):

$$K_{\mathrm{d}} - K_{\mathrm{m}} = \frac{1}{3}(K' - K_{\mathrm{m}})\frac{3K_{\mathrm{d}} + 4\mu_{\mathrm{m}}}{3K_{\mathrm{m}} + 4\mu_{\mathrm{m}}}\sum_{l}\phi_l T_1(\alpha_l), \tag{3}$$

$$G_{\mathrm{d}} - G_{\mathrm{m}} = \frac{1}{5}(G' - G_{\mathrm{m}}) \times \frac{6G_{\mathrm{d}}(K_{\mathrm{m}} + 2G_{\mathrm{m}}) + G_{\mathrm{m}}(9K_{\mathrm{m}} + 8G_{\mathrm{m}})}{5G_{\mathrm{m}}(3K_{\mathrm{m}} + 4G_{\mathrm{m}})}\sum_{l}\phi_l F(\alpha_l), \tag{4}$$

where K_{d}, K_{m}, and K' denote the bulk moduli of the rock frame, matrix, and pore-filling material, respectively, while G_{d}, G_{m}, and G' correspond to their shear moduli. φ_l represents the volume fraction of the l-th pore-filling phase, and α_l denotes the pore aspect ratio as Equation (5):

$$F(\alpha_l) = T_2(\alpha_l) - \frac{T_1(\alpha_l)}{3}. \tag{5}$$

The K–T model is applicable when the ratio of porosity to pore aspect ratio is much smaller than 1. Under this condition, the rock matrix can be treated as a continuous background medium, while pores act as sparse perturbing inclusions that modify the effective elastic moduli. It is important to note that, in the initial porosity-inclusion step, both the bulk and shear moduli of the pore-filling phase are set to zero, effectively assuming a dry rock frame with no fluid saturation. Carbonate reservoirs exhibit highly complex pore systems, including intergranular and intercrystalline pores as well as secondary features such as dissolution-enlarged pores, fractures, and vugs. To capture the combined influence of porosity on seismic velocities and acoustic impedance, we employ the Gassmann fluid-substitution equations. According to Gassmann's theory, fluid saturation alters the effective elastic properties of the rock frame. Using the Gassmann relations, the elastic moduli and seismic velocities of fluid-saturated rocks can be written as functions of the dry-frame moduli, mineral matrix properties, and the bulk modulus of the pore fluid, as shown in Equation (6):

$$K_s = K_d + \frac{\left(1 - \frac{K_d}{K_{\mathrm{m}}}\right)^2}{\frac{\phi}{K_f} + \frac{1-\phi}{K_{\mathrm{m}}} - \frac{K_d}{K_{\mathrm{m}}^2}}, G_s = G_d, \tag{6}$$

where K_s represents the bulk modulus of the saturated rock, G_s is the shear modulus of the saturated rock, and K_f denotes the bulk modulus of the pore fluid.

The bulk modulus and density of the saturating fluid can be computed using Equation (7):

$$K_f = \left(\frac{1 - S_w}{K_g} + \frac{S_w}{K_w}\right)^{-1}, \rho_f = (1 - S_w)\rho_{hc} + S_w\rho_w, \quad (7)$$

where S_w denotes the water saturation; K_g and K_w denote the bulk moduli of gas and water, respectively; ρ_w is the density of water; ρ_g is the density of gas; and ρ_f represents the density of the saturated fluid.

Ultimately, the elastic properties of the saturated rock can be described using Equation (8):

$$\begin{aligned} V_P &= \sqrt{\left(K_s + \tfrac{4}{3}G_s\right)/\rho} \\ V_S &= \sqrt{G_{sat}/\rho} \\ \rho &= \rho_m(1 - \phi) + \rho_f\phi \end{aligned}. \quad (8)$$

2.2. A Rock-Physics-Constrained Deep Learning Inversion Framework

In traditional post-stack seismic data, amplitude variation with offset (AVO) is largely diminished or even eliminated during the stacking process, substantially reducing the sensitivity of the data to lithologic and fluid changes [32,33]. Relying solely on post-stack impedance inversion and then inferring porosity through rock-physics transforms tends to introduce compounded uncertainties and cumulative errors, ultimately lowering the accuracy and credibility of the predictions. In contrast, integrating seismic inversion with rock-physics constraints and incorporating high-resolution well-log information allows a synergistic fusion of the seismic data's large-scale continuity and the detailed local resolution of well measurements. This hybrid inversion strategy—combining physics-based modeling with data-driven learning—not only compensates for the information loss inherent in post-stack data but also greatly enhances the stability and resolution of porosity prediction, offering a more robust foundation for the fine characterization of complex reservoirs. This workflow typically relies on the seismic convolution model to generate synthetic post-stack traces, ensuring physical consistency and geological plausibility in the inversion. The procedure is formulated in Equation (9):

$$d = W * R, \quad (9)$$

where W represents the seismic wavelet and R denotes the reflectivity series, which for post-stack seismic data can be written as Equation (10):

$$R = \frac{\rho_2 V_{P2} - \rho_1 V_{P1}}{\rho_2 V_{P2} + \rho_1 V_{P1}}, \quad (10)$$

where ρ denotes the medium density, and Vp denotes the P-wave velocity. Subscripts 1 and 2 correspond to the upper and lower layers, respectively.

Data-driven porosity inversion has become an increasingly popular reservoir-parameter prediction technique, stimulated by the rapid advancements in deep learning over recent years. The core idea is to exploit the powerful nonlinear representation ability of deep neural networks to automatically learn the complex mapping between seismic data and porosity. During training, post-stack seismic amplitude traces extracted from the 3D seismic volume are used as inputs, while high-resolution porosity logs serve as supervision labels. The network parameters are updated iteratively through backpropagation, driving the predicted porosity to converge toward the true log measurements. The training objective is to minimize the discrepancy between predicted and logged porosity, typically

formulated through a loss function that governs the optimization process, as expressed in Equation (11):

$$\mathcal{L} = \frac{1}{N}\sum_{i=1}^{N}\left[\phi_{\text{pred}}(i) - \phi_{\text{true}}(i)\right]^2, \tag{11}$$

where $\phi_{\text{pred}}(i)$ represents the network-predicted porosity, $\phi_{\text{true}}(i)$ is the porosity measured from well logs, and N denotes the total number of training samples. Through iterative parameter updates, the loss function is driven toward its minimum, enabling a high-accuracy mapping between seismic attributes and porosity.

Within a data-driven inversion workflow, the porosity curve predicted by the network is not the final result but serves as a crucial input for subsequent rock-physics modeling. Specifically, integrating the predicted porosity with well-log parameters—such as clay content and water saturation—enables the construction of quantitative relationships between rock-physics properties and elastic parameters such as P-wave velocity, S-wave velocity, and density. These relationships allow the generation of full elastic-parameter logs, which can then be used to perform seismic forward modeling and produce synthetic seismograms comparable to field seismic data. During inversion, updating model parameters solely by minimizing the misfit between observed and synthetic seismic data can indeed improve data matching, but often leads to overfitting or excessive oscillations in the inversion results, undermining geological plausibility. To address this issue, regularization terms are typically incorporated into the objective function to impose smoothness constraints on model parameters. This enhances lateral continuity and stabilizes depositional trends, ultimately yielding more robust, stable, and geologically consistent inversion results.

Finally, the overall loss function governing the inversion network can be defined as Equation (12):

$$\mathcal{L}_{\text{total}} = \underbrace{||\, d_{\text{obs}} - d_{\text{syn}} \,||^2 + \lambda_1 ||\, \nabla m \,||^2}_{\mathcal{L}1} + \underbrace{\lambda_2 ||\, \phi_{\text{pred}} - \phi_{\text{true}} \,||^2}_{\mathcal{L}2}, \tag{12}$$

where d_{obs} refers to the observed seismic data, while d_{syn} represents the synthetic seismogram produced through forward modeling of the inversion model. In Equation (12), $\mathcal{L}1$ represents the inversion term constrained by post-stack seismic data, where ∇m denotes the smoothness term applied to the predicted porosity model, and λ_1 is the corresponding smoothing coefficient. The term $\mathcal{L}2$ represents the misfit between the porosity derived from well logs and the predicted porosity, corresponding to the data-driven component of the proposed method. The coefficient λ_2 controls the relative contribution of the data-driven term in the overall optimization during the experiments.

This study develops a Physics-Constrained TransUNet architecture by embedding Transformer-based self-attention modules into the conventional U-Net encoder–decoder framework. The overall architecture consists of an Encoder built from multiple convolutional and down-sampling blocks, designed to extract multi-scale local features from seismic attributes; A Transformer bottleneck module, which leverages self-attention to capture long-range dependencies and spatial patterns associated with fracture–karst composite systems; A Decoder that performs feature up-sampling and spatial reconstruction via transposed convolutions, while incorporating skip connections to preserve shallow-level details. When the rock-physics modeling module is embedded into the network, the resulting overall architecture is illustrated in Figure 1.

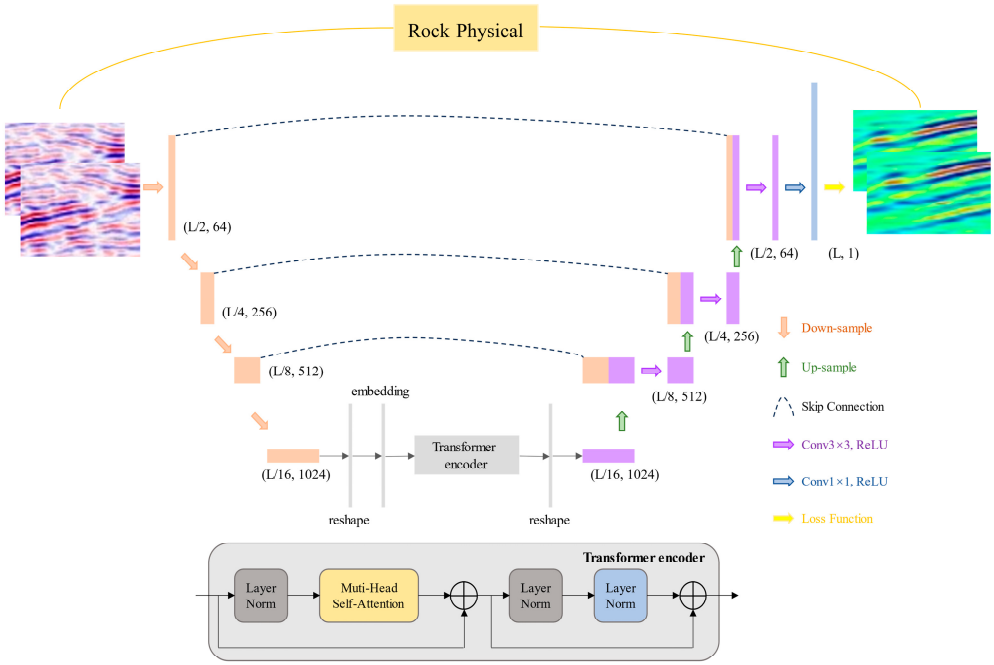


Figure 1. Physics-Constrained TransUNet framework integrating rock-physics modeling and Transformer bottleneck.

3. Results

3.1. Study Area Overview

The Tarim Basin represents one of China's most significant provinces for deep and ultra-deep marine carbonate exploration. In its northern sector, thick platform carbonates of the Middle–Lower Ordovician are extensively developed, forming a core target interval for deep hydrocarbon reserve growth and stable production. The XX well block lies on the western flank of the Tabei Uplift in northern Tarim Basin, situated within a NE-trending strike–slip system between the Halaha–Tang Depression and the Shuntogole Low Uplift. Bounded by the Luntai Uplift to the north, the Manjaer Depression to the south, and the Yingmaili High to the west, it constitutes one of the most prospective deep hydrocarbon accumulation zones in the western Tabei Uplift.

The Middle–Lower Ordovician interval comprises thick platform limestones, dolomites, and their diagenetic derivatives. Overprinting effects of facies variations, diagenesis, hydrothermal alteration, and multiple tectonic episodes have produced a complex reservoir architecture characterized by multi-scale, multi-type fractures, pores, and vugs. Multiphase strike–slip and transpressional deformation has led to the widespread development of "fault–dissolution–vug" composite reservoirs along major and subsidiary faults, forming a typical fault-controlled fracture–vug system. Hydrothermal dissolution along steep, deep-seated faults has produced extensive collapse structures, vertical caverns, and characteristic bead-like strong reflections within the Yijianfang and upper Yingshan formations—representing the dominant high-yield reservoir types in the region. Reservoir burial depths commonly exceed 7000 m in the XX block, with some wells deeper than 8000 m, exhibiting the typical "ultra-deep, ultra-high pressure, and ultra-high temperature" attributes. Intense tectonic–karst overprinting has produced extreme heterogeneity, with abrupt lateral and vertical changes in porosity, permeability, and fracture intensity. High-output wells occur mainly within fault–karst composite belts and fracture–vug zones, whereas nearby wells may be low-yielding or ineffective, complicating efforts to delineate reservoir connectivity, effective thickness, and spatial distribution.

The FI7 fault belt of the XX block lies within a prime segment of the Tabei strike–slip system and represents a key target zone for reserve enhancement and production in fault-controlled fracture–vug carbonate reservoirs. Numerous wells have yielded high oil and gas flows from Ordovician fault-controlled fracture–vug reservoirs, indicating that the FI7 zone benefits from favorable hydrocarbon charge, efficient fault-conduit pathways, and strongly developed fracture–vug storage space. However, the FI7 fault belt exhibits pronounced segmentation, with substantial variations in fault activity, dip angle, linkage patterns, and karst modification along the fault plane. These factors lead to highly complex reservoir boundaries and intricate internal cave–fracture–pore systems, as well as secondary faults acting as fluid conduits or barriers, representing major sources of uncertainty in reservoir prediction.

The available geophysical dataset comprises high-resolution 3D seismic data over the FI7 belt, supplemented by sparse well logs, mud logs, and test data from several ultra-deep wells. Sparse well control and log distortions caused by high-temperature, high-pressure, and unstable borehole conditions further reduce the spatial continuity and quantitative reliability of porosity prediction using single-attribute or conventional inversion approaches. The challenge is even greater in fracture–vuggy carbonates, where seismic signatures frequently include bead-like strong reflections, chaotic events, and localized energy anomalies, further complicating porosity inversion. Figure 2 presents a representative post-stack seismic section, in which large bead-like strong reflections along the fault trace reveal vertical vug/cave accumulations and collapse features. Considering the intricate tectonic–sedimentary–karst coupling and data limitations, this study focuses on the fracture–vuggy carbonate reservoirs of the FI7 fault belt, systematically investigating the development mechanisms and seismic response characteristics of "fault–dissolution–vug" composite systems. By incorporating rock-physics constraints and integrating sparse well-log porosity data with multi-attribute seismic information, we establish a high-resolution porosity prediction and reservoir-structure characterization framework tailored for ultra-deep carbonates. This provides robust technical support for sweet-spot evaluation, reservoir geological modeling, and development planning.

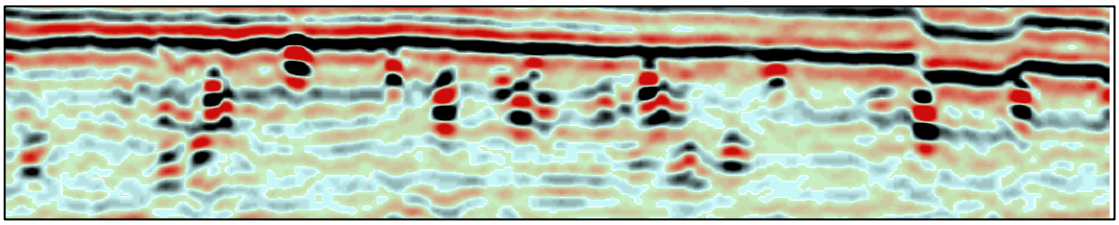


Figure 2. Representative Post-Stack Seismic Profile of a Selected Line in the Study Area.

3.2. Evaluation of Porosity Prediction Performance

The study area is covered by a 3D seismic survey, and this work utilizes a 3D seismic dataset acquired across the entire block. Beyond standard processing steps—static correction, amplitude recovery, denoising, multiple suppression, deconvolution, velocity analysis, and prestack migration—the dataset was further enhanced using structural-oriented filtering, spectral optimization, and imaging-quality improvement techniques. These steps significantly improved the continuity and resolution of deep reflectors, yielding a high-SNR, well-imaged 3D post-stack seismic volume suitable for subsequent attribute extraction, inversion, and detailed reservoir characterization. Figure 3 illustrates the 3D seismic coverage and the distribution of representative wells across the study area, providing constraints on fault geometry and reservoir lateral heterogeneity. The straight line marks a selected inter-well profile that highlights the seismic response between wells and the lateral variations in

the target interval. Figure 4 presents the post-stack seismic section along this inter-well line. Major fault structures and strong-amplitude reflections of the target reservoir are clearly imaged, providing essential support for well–seismic calibration, seismic facies analysis, and subsequent reservoir prediction. The inter-well line is oriented along the main controlling fault and the dominant reservoir trend, comprising 2081 CDPs. Figure 4a displays CDPs 1–1040, while Figure 4b covers CDPs 1401–2081. Four wells are positioned along the line at evenly distributed CDP locations, as summarized in Table 1. The spatial arrangement of wells along the profile effectively captures faulted zones and favorable reservoir belts, while representing different structural settings and reservoir distributions. This configuration offers strong constraints for well–seismic calibration, facies interpretation, and the training and validation of porosity prediction models.

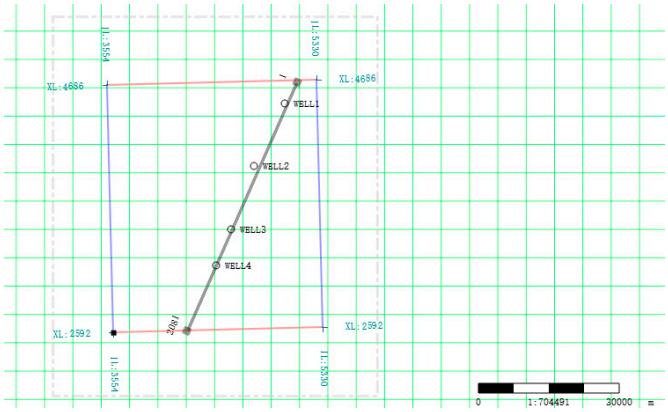


Figure 3. Schematic Map of the Study Area.

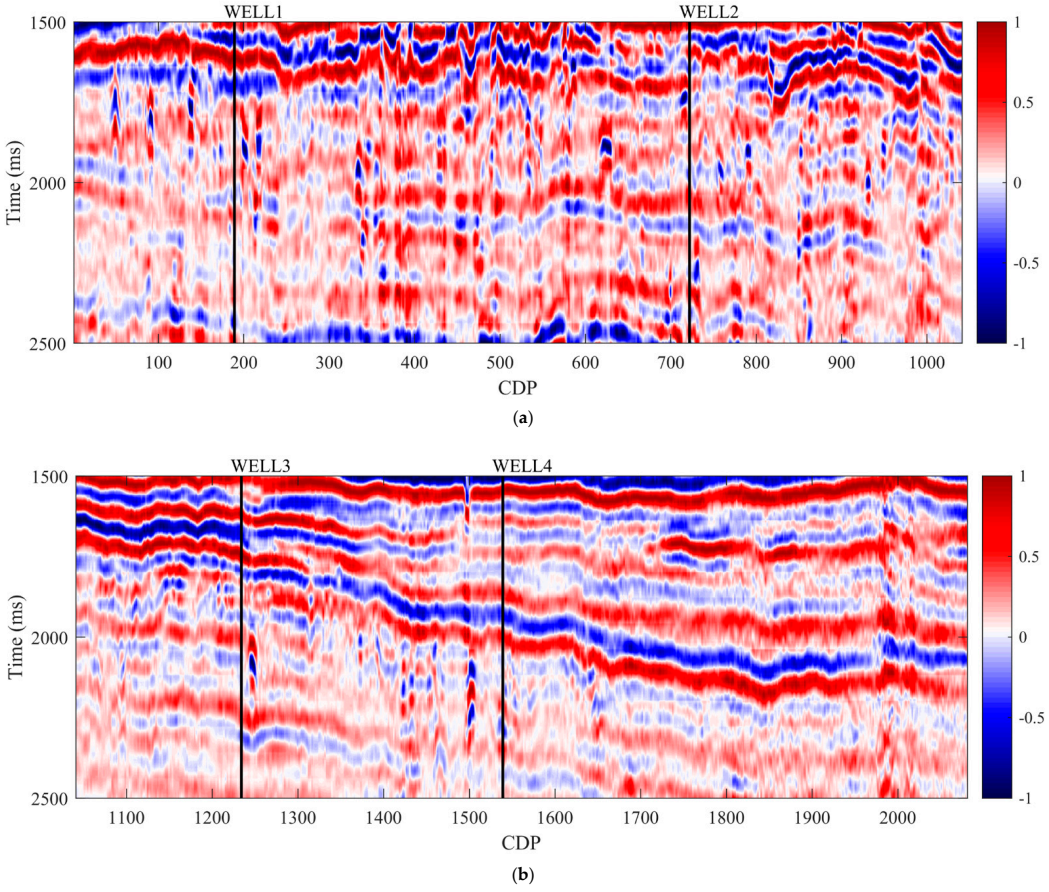


Figure 4. Post-stack Seismic Section of the Inter-well Line (CDP 1–2081): (**a**) CDP 1–1040; (**b**) CDP 1041–2081.

Table 1. Well-to-CDP Position Table.

WELL	WELL1	WELL2	WELL3	WELL4
CDP	189	722	1234	1539

The well logs from WELL1, WELL2, and WELL3 together with their corresponding near-well seismic traces were used to construct the training dataset, whereas WELL4 served as the blind-well validation dataset. Figure 5 illustrates the porosity logs from the four wells. Rock-physics modeling also requires water saturation and clay content; however, as this study focuses primarily on porosity prediction, these parameters were assigned layer-wise empirical values derived from statistical analyses of logs within the study area. Comparison of predicted porosity with core data shows that the model responds strongly within vuggy intervals. For core porosity exceeding 6%, the predictions reliably capture the associated density drop and the increase in acoustic slowness. In intervals affected by borehole enlargement (CALI anomalies), the incorporation of deep-learning feature construction and derivative-based constraints prevents spurious deviations, demonstrating the strong robustness of the predictions. Furthermore, in sections showing abrupt density drops or rapid increases in acoustic slowness, the model consistently identifies fracture–vuggy reservoir intervals, effectively avoiding the "over-smoothed misclassification" issue typical of purely data-driven models. The Physics-Constrained TransUNet was trained through iterative optimization on the training dataset, and the loss-function convergence curve is presented in Figure 6. As training proceeded, the loss value decreased steadily and stabilized at around epoch 30, indicating that the network had effectively learned the nonlinear seismic–porosity mapping. The embedded physics-based constraints helped suppress overfitting and improved the geological plausibility of the inversion results. Once convergence was achieved, the optimal network parameters were selected for predicting porosity in the target well.

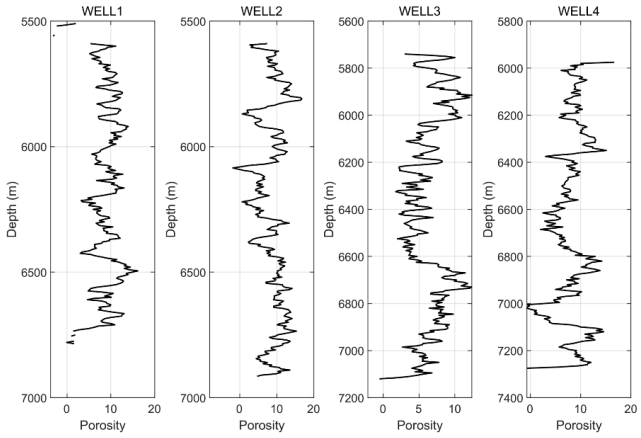


Figure 5. Porosity Logs of the Four Wells Used in the Study.

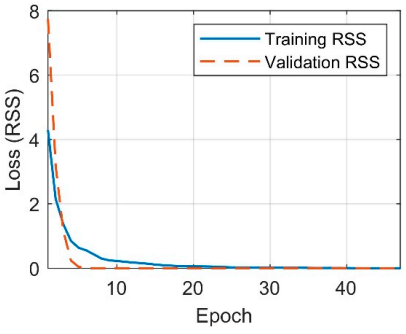


Figure 6. Evolution of Training Loss for the Physics-Constrained TransUNet.

The trained model was applied to the blind well WELL4, and the corresponding porosity prediction results obtained using the proposed Physics-Constrained TransUNet method are shown in Figure 7. The predicted porosity log exhibits good agreement with the interpreted well-log porosity in both overall trends and local variations, accurately delineating high- and low-porosity intervals of the reservoir. In particular, the method demonstrates strong conformity within key reservoir sections, indicating its capability to capture relevant geological features. For comparison, Figure 8 presents the porosity prediction results derived from an empirical formula commonly used for carbonate reservoirs. A comparison between Figures 7 and 8 shows that, although the empirical approach provides a reasonable approximation of the general porosity trend, it tends to produce overly smooth results and fails to adequately resolve local fluctuations and small-scale heterogeneity. In contrast, the proposed method not only preserves the large-scale trend but also achieves superior recovery of fine-scale porosity variations, better reflecting the complex pore structure of fracture–vuggy carbonate reservoirs.

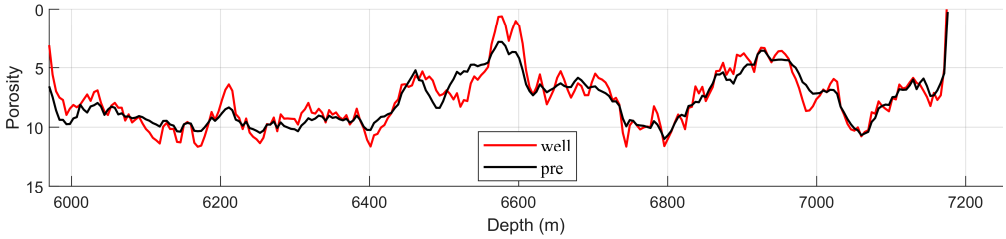


Figure 7. Porosity Prediction Results for WELL4 Using the Physics-Constrained TransUNet Model.

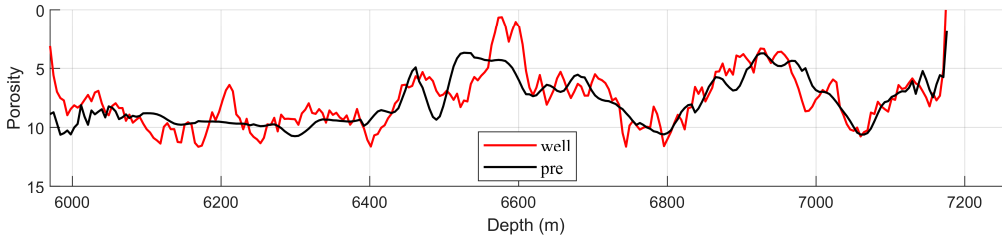


Figure 8. Porosity Prediction Results for WELL4 Using the empirical formula.

To quantitatively evaluate the prediction performance, Table 2 reports the Pearson correlation coefficient (PCC), mean relative error (MRE), and coefficient of determination (R^2) metrics for both the proposed method and the empirical approach at WELL4. The results indicate that the Physics-Constrained TransUNet consistently outperforms the empirical method across all evaluation metrics, demonstrating improved prediction accuracy and stability. Furthermore, Table 3 compares the correlations between measured porosity logs and elastic parameters (P-wave velocity, S-wave velocity, and density) with those between predicted porosity and the corresponding elastic parameters. The comparable correlation patterns observed in these two cases indicate that the predicted porosity retains physically consistent relationships with elastic properties. This consistency further validates the effectiveness and geological reliability of the proposed method from a rock-physics perspective.

Table 2. Quantitative assessment of inversion performance.

Method	PCC	MRE (%)	R^2
TransUNet	0.9306	11.47	0.8514
Empirical formula	0.8845	16.79	0.7749

Table 3. Pearson correlation coefficients (PCCs) between predicted and elastic parameters.

Method	PCC-vp	PCC-vs	PCC-den
pre	−0.55	−0.70	−0.48
well	−0.63	−0.75	−0.49

Applying the trained Physics-Constrained TransUNet model to the seismic data along the selected inter-well line yields the porosity prediction section shown in Figure 9. Figure 10 presents the porosity prediction slice extracted from the main target interval. The results demonstrate that the proposed model exhibits clear advantages in predicting fracture–vuggy carbonate reservoirs. The predicted section captures the lateral continuity of porosity with high clarity and effectively identifies highly heterogeneous features such as fracture–dissolution composite bodies that exhibit significant scale variations. In complex fracture–vug development zones, the model accurately delineates the position, extent, and morphology of porosity anomalies, outperforming traditional attribute stacking and conventional inversion techniques by a substantial margin. Overall, the model demonstrates strong sensitivity and stability in identifying fracture–vuggy reservoirs and characterizing porosity distributions, offering a robust technical foundation for the fine-scale evaluation of carbonate reservoirs.

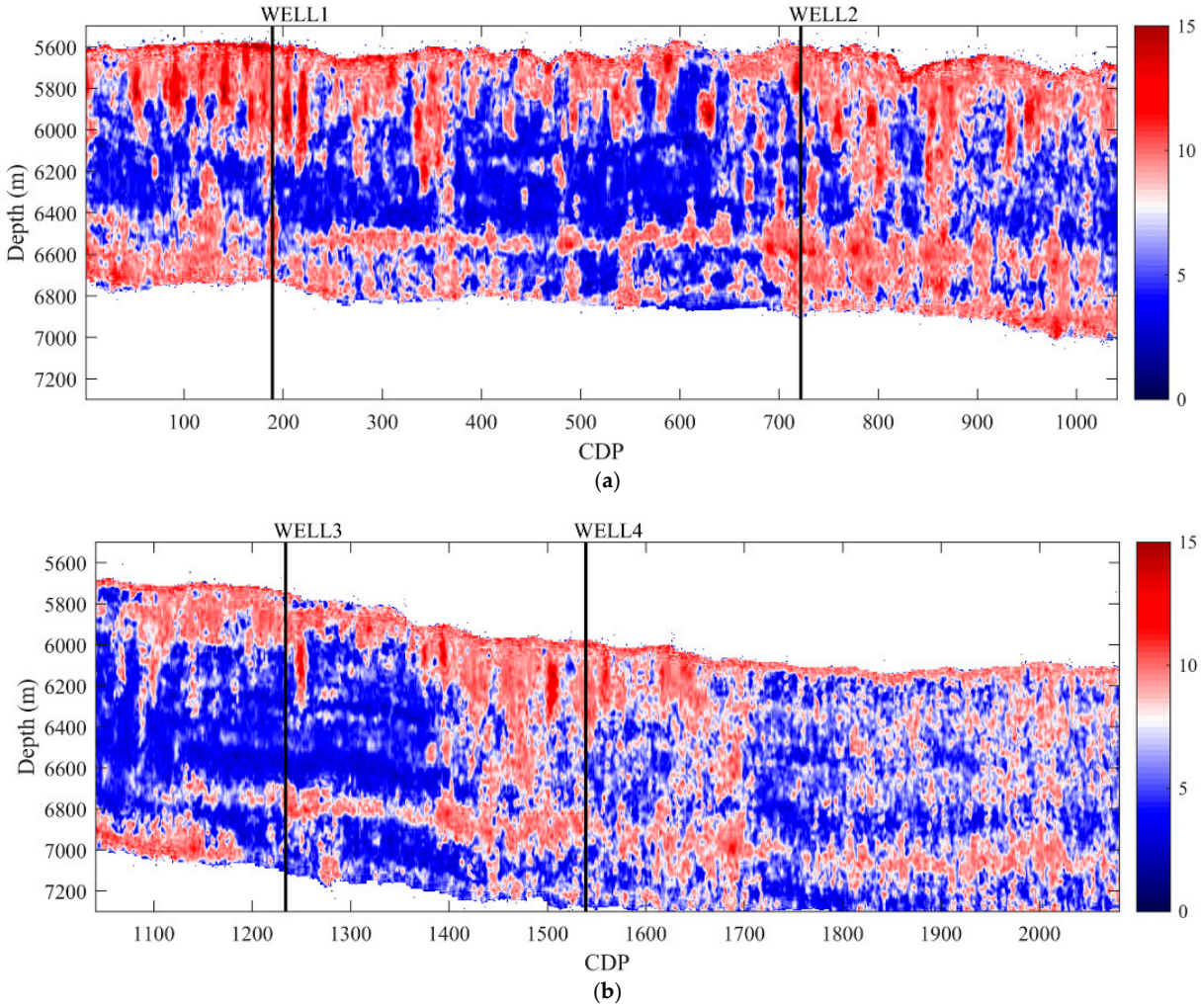


Figure 9. Porosity Prediction Profile Generated by the Physics-Constrained TransUNet Model Along the Inter-well Line: (**a**) CDP 1–1040; (**b**) CDP 1041–2081.

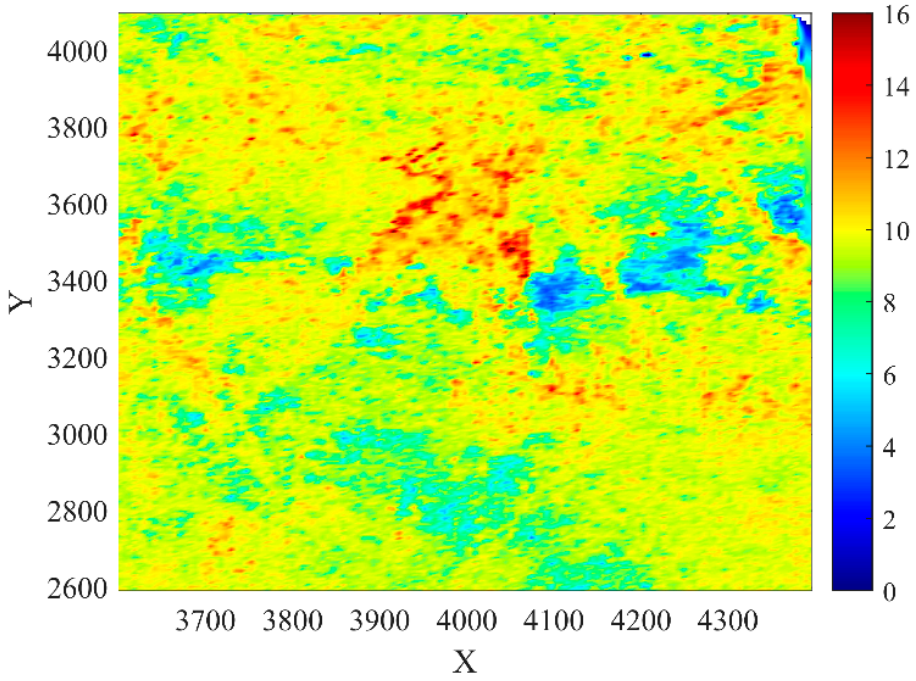


Figure 10. Porosity Distribution Slice Across the Main Target Interval.

4. Discussion

The Physics-Constrained TransUNet proposed in this work exhibits strong predictive performance in ultra-deep fracture–vuggy carbonate reservoirs. However, several aspects related to its theoretical foundations, geological applicability, and practical deployment warrant further examination. Methodologically, the incorporation of rock-physics constraints narrows the solution space of the deep-learning model, enabling predictions that more closely follow realistic geological patterns at both large and fine scales. In settings with sparse well control and strong heterogeneity, purely data-driven models often struggle with unstable inter-well extrapolation and blurred porosity transitions. In contrast, the physical constraints impose a physically meaningful evolution pathway for elastic responses, enhancing lateral continuity and stability near fracture–karst systems. It is important to acknowledge that rock-physics models rely on idealized assumptions. Features such as anisotropic pore systems, variable fracture apertures, and scale effects of large karst cavities are difficult to capture accurately. As a result, deviations may still arise near extreme geological bodies such as large collapse zones or giant caverns. Moreover, because logging data in ultra-deep carbonate reservoirs are sparse, key parameters such as water saturation and clay content often rely on empirical assignments. This inevitably weakens the rigor of the physical constraints and may introduce additional uncertainty.

Regarding the coordination between data characteristics and network architecture, TransUNet effectively integrates CNNs' local feature extraction with Transformers' long-range dependency modeling, providing advantages in identifying complex fracture–vug systems. Nevertheless, inherent limitations of post-stack seismic—restricted bandwidth, limited resolution, and wavelet instability—mean that small-scale features at depth may still be inadequately resolved. Although structural-oriented filtering, spectral enhancement, and other processing techniques have improved seismic data quality, the fundamental physical limitations of seismic imaging continue to restrict prediction accuracy. Furthermore, although physical constraints mitigate overfitting, deep-learning networks still rely on adequate near-well training data. In areas with extremely sparse well control, network expressiveness becomes limited—a widespread challenge in deep carbonate reservoir studies.

In this study, a multi-well training and validation strategy was adopted to better reflect realistic field-application scenarios under limited well control. Multiple wells within the study area were jointly used to construct the training dataset, while an additional well (WELL4) was reserved exclusively as an independent blind well for generalization assessment. This strategy allows the model to learn shared seismic–porosity relationships across different wells while providing a more stringent and practical evaluation of inter-well extrapolation capability than random sample-level splitting alone. Given the strong heterogeneity of fracture–vuggy carbonate reservoirs and the limited number of available wells, this approach offers a reasonable balance between training robustness and validation reliability. Potential extensions, such as systematic cross-validation across wells, may further enhance statistical representativeness when more well data become available.

Overall, the proposed collaborative inversion framework substantially enhances both the geological plausibility and spatial continuity of porosity predictions, though opportunities for further improvement remain. Future research may advance in three directions: (1) incorporating digital rock models or multi-scale CT imaging to better capture the true complexity of multi-type pore structures; (2) integrating fracture- and pore-sensitive attributes—such as pre-stack AVAZ, spectral attenuation, and elastic impedance—into the dataset to improve the model's ability to resolve complex reservoirs; (3) embedding uncertainty quantification techniques within the deep-learning framework to assess prediction confidence, offering more interpretable support for reservoir risk assessment and development planning.

In summary, integrating physical constraints with deep learning provides a promising new pathway for porosity prediction in fracture–vug carbonate reservoirs. The approach shows significant potential, yet continued progress is needed in improving rock-physics realism, enhancing model generalization, and better integrating multi-source geological and geophysical data.

5. Conclusions

This study addresses key challenges in the XX well block of the Tarim Basin—strong heterogeneity in fracture–vuggy carbonate reservoirs, sparse well control, and limited seismic resolution—by developing a Physics-Constrained TransUNet framework that combines rock-physics constraints with the representational advantages of deep learning. The workflow begins by constructing a rock-physics model tailored for marine carbonates, integrating mineral composition, pore structure, water saturation, and fluid properties into a unified quantitative framework that ensures physical consistency between porosity, elastic properties, and seismic responses. These rock-physics priors, together with regularization terms and well-log supervision, are embedded within the TransUNet architecture to form a hybrid "physics-driven plus data-driven" collaborative inversion framework. Case study results demonstrate stable convergence of the model and accurate delineation of key reservoir features—including vugs, fractures, and high-porosity zones. Compared with traditional attribute-based methods and conventional inversion, the proposed approach achieves superior well-log matching and markedly improved lateral continuity between wells. The predicted inter-well section and target-interval porosity slice further confirm the model's sensitivity to fault–dissolution–vug systems and its strong capability in identifying complex reservoir architectures, favorable reservoir zones, and potential sweet spots. In summary, the physics-constrained deep-learning framework significantly enhances both the accuracy and geological plausibility of porosity prediction in fracture–vuggy carbonate reservoirs, offering a robust and scalable solution for fine characterization and development planning in ultra-deep, complex reservoir settings.

https://doi.org/10.3390/pr14030520

Author Contributions: Conceptualization, H.Z. and X.D.; methodology, H.Z.; software, H.Z.; validation, H.Z., X.D. and Y.L.; formal analysis, H.Z.; investigation, H.Z.; resources, Z.L. and Y.M.; data curation, H.Z. and Y.M.; writing—original draft preparation, H.Z.; writing—review and editing, H.Z., X.D. and Z.J.; visualization, H.Z.; supervision, X.D.; project administration, X.D.; funding acquisition, X.D. All authors have read and agreed to the published version of the manuscript.

Funding: This research was funded by National Technology Project of China National Petroleum Corporation (2023ZZ16YJ02), Science and Technology Project of PetroChina Tarim Oilfield Company (T202408) and Major Science and Technology Project of the Autonomous Region (2024A01010).

Institutional Review Board Statement: Not applicable.

Informed Consent Statement: Not applicable.

Data Availability Statement: The original contributions presented in this study are included in the article. Further inquiries can be directed to the corresponding author.

Conflicts of Interest: Authors Haitao Zhao, Xingliang Deng, Zhengyang Li and Yuan Ma were employed by PetroChina Tarim Oilfield Company and its affiliated research institutes. The remaining authors were employed by an academic institution. The authors declare that the research was conducted in the absence of any commercial or financial relationships that could be construed as a potential conflict of interest. The authors declare that this study received funding from China National Petroleum Corporation and PetroChina Tarim Oilfield Company. The funder was not involved in the study design, data collection, analysis or interpretation, the writing of the manuscript, or the decision to submit it for publication.

Abbreviations

The following abbreviations are used in this manuscript:

CNN	Convolutional neural network
LSTM	Long short-term neural network
AVO	Amplitude variation with offset
POR	Porosity
CDP	Common Depth Point
AVAZ	Amplitude Variation with Azimuth

References

1. Liu, B.; Yang, F.; Zhang, G.; Zhao, L.; Liu, B.; Yang, F.; Zhang, G.; Zhao, L. Pre-Stack Fracture Prediction in an Unconventional Carbonate Reservoir: A Case Study of the M Oilfield in Tarim Basin, NW China. *Energies* **2024**, *17*, 2061. [CrossRef]
2. Liu, J.; Zhao, L.; Xu, M.; Zhao, X.; You, Y.; Geng, J. Porosity Prediction from Prestack Seismic Data via Deep Learning: Incorporating a Low-Frequency Porosity Model. *J. Geophys. Eng.* **2023**, *20*, 1016–1029. [CrossRef]
3. Adam, A.; Swennen, R.; Abdulghani, W.; Abdlmutalib, A.; Hariri, M.; Abdulraheem, A. Reservoir Heterogeneity and Quality of Khuff Carbonates in Outcrops of Central Saudi Arabia. *Mar. Pet. Geol.* **2018**, *89*, 721–751. [CrossRef]
4. Abdolmaleki, J.; Tavakoli, V.; Asadi-Eskandar, A. Sedimentological and Diagenetic Controls on Reservoir Properties in the Permian–Triassic Successions of Western Persian Gulf, Southern Iran. *J. Pet. Sci. Eng.* **2016**, *141*, 90–113. [CrossRef]
5. Teillet, T.; Fournier, F.; Zhao, L.; Borgomano, J.; Hong, F. Geophysical Pore Type Inversion in Carbonate Reservoir: Integration of Cores, Well Logs, and Seismic Data (Yadana Field, Offshore Myanmar). *Geophysics* **2021**, *86*, B149–B164. [CrossRef]
6. Pan, X.; Zhang, G.; Yin, X. Amplitude Variation with Offset and Azimuth Inversion for Fluid Indicator and Fracture Weaknesses in an Oil-Bearing Fractured Reservoir. *Geophysics* **2019**, *84*, N41–N53. [CrossRef]
7. Guo, Q.; Ba, J.; Luo, C. Seismic Rock-Physics Linearized Inversion for Reservoir-Property and Pore-Type Parameters with Application to Carbonate Reservoirs. *Geoenergy Sci. Eng.* **2023**, *224*, 211640. [CrossRef]
8. Deng, Z.; Zhou, D.; Dong, H.; Huang, X.; Wei, S.; Kang, Z. Deep Learning for Predicting Porosity in Ultra-Deep Fractured Vuggy Reservoirs from the Shunbei Oilfield in Tarim Basin, China. *Sci. Rep.* **2024**, *14*, 29605. [CrossRef]
9. Wang, J.; Deng, J.; Xia, H.; Yan, L. Rock Physics Characteristics and Their Control Factors of Carbonate in Different Sedimentary Microfacies of the Yingshan Formation, Gucheng Area, Tarim Basin. *J. Geophys. Eng.* **2023**, *20*, 1308–1321. [CrossRef]
10. Ding, Y.; Du, Q.; Fu, L.; Jian, S. Reliability Analysis of Seismic Attribute in the Detection of Fault-Karst. *Interpretation* **2020**, *8*, SP61–SP70. [CrossRef]

11. Sun, S.Z.; Wang, H.; Liu, Z.; Li, Y.; Zhou, X.; Wang, Z. The Theory and Application of DEM-Gassmann Rock Physics Model for Complex Carbonate Reservoirs. *Lead Edge* **2012**, *31*, 152–158. [CrossRef]
12. Ba, J.; Xu, W.; Fu, L.; Carcione, J.M.; Zhang, L. Rock Anelasticity Due to Patchy Saturation and Fabric Heterogeneity: A Double Double-porosity Model of Wave Propagation. *J. Geophys. Res. Solid Earth* **2017**, *122*, 1949–1976. [CrossRef]
13. Chen, S.; Wang, Y.; Guo, J.; He, Q.; Yin, X. Multi-Scale Evaluation of Fractured Carbonate Reservoir and Its Implication to Sweet-Spot Optimization: A Case Study of Tazhong Oilfield, Central Tarim Basin, China. *Energy Rep.* **2021**, *7*, 2976–2988. [CrossRef]
14. Hendry, J.; Burgess, P.; Hunt, D.; Janson, X.; Zampetti, V. Seismic Characterization of Carbonate Platforms and Reservoirs: An Introduction and Review. In *Geological Society, London, Special Publications*; The Geological Society of London: London, UK, 2021; Volume 509, pp. 1–28. [CrossRef]
15. Wang, Y.; Xie, P.; Zhang, H.; Liu, Y.; Yang, A. Fracture-Vuggy Carbonate Reservoir Characterization Based on Multiple Geological Information Fusion. *Front. Earth Sci.* **2024**, *11*, 1345028. [CrossRef]
16. Li, Z.; Li, H.; Liu, J.; Deng, G.; Gu, H.; Yan, Z. 3D Seismic Intelligent Prediction of Fault-Controlled Fractured-Vuggy Reservoirs in Carbonate Reservoirs Based on a Deep Learning Method. *J. Geophys. Eng.* **2024**, *21*, 345–358. [CrossRef]
17. Pramanik, A.G.; Singh, V.; Vig, R.; Srivastava, A.K.; Tiwary, D.N. Estimation of Effective Porosity Using Geostatistics and Multiattribute Transforms: A Case Study. *Geophysics* **2004**, *69*, 352–372. [CrossRef]
18. Song, Z.; Li, S.; He, S.; Yuan, S.; Wang, S. Gas-Bearing Prediction of Tight Sandstone Reservoir Using Semi-Supervised Learning and Transfer Learning. *IEEE Geosci. Remote Sens. Lett.* **2022**, *19*, 1–5. [CrossRef]
19. Wu, B.; Meng, D.; Zhao, H. Semi-Supervised Learning for Seismic Impedance Inversion Using Generative Adversarial Networks. *Remote Sens.* **2021**, *13*, 909. [CrossRef]
20. Liu, J.; Gui, Z.; Gao, G.; Li, Y.; Wei, Q.; Liu, Y. Predicting Shear Wave Velocity Using a Convolutional Neural Network and Dual-Constraint Calculation for Anisotropic Parameters Incorporating Compressional and Shear Wave Velocities. *Processes* **2023**, *11*, 2356. [CrossRef]
21. Liu, Z.; Chen, X.; Li, J.; Hou, S.; Li, Z.; Liu, G. Robust Weakly Supervised Learning Pre-Stack Multi-Trace Seismic Inversion. *IEEE Trans. Geosci. Remote Sens.* **2023**, *62*, 1–11. [CrossRef]
22. Dang, Y.; Zhang, Y.; Wu, B.; Li, H.; Gao, J. An Efficient Method of Predicting S-Wave Velocity Using Sparse Gaussian Process Regression for a Tight Sandstone Reservoir. *J. Appl. Geophys.* **2024**, *229*, 105480. [CrossRef]
23. Feng, G.; Liu, W.-Q.; Yang, Z.; Yang, W. Shear Wave Velocity Prediction Based on 1DCNN-BiLSTM Network with Attention Mechanism. *Front. Earth Sci.* **2024**, *12*, 1376344. [CrossRef]
24. Qi, Y.; Luo, S.; Tang, S.; Ruan, J.; Gao, D.; Liu, Q.; Li, S. Prediction of Carbonate Reservoir Porosity Based on CNN-BiLSTM-Transformer. *Appl. Sci.* **2025**, *15*, 3443. [CrossRef]
25. Yan, B.; Zhao, J.; Peng, K.; Qian, L.; Li, M.; Pan, R. 3D Karst Cave Recognition Using TransUnet with Dual Attention Mechanisms in Seismic Images. *Geophysics* **2025**, *90*, IM133–IM143. [CrossRef]
26. Wang, J.; Cao, J.; Yuan, S. Deep Learning Reservoir Porosity Prediction Method Based on a Spatiotemporal Convolution Bi-Directional Long Short-Term Memory Neural Network Model. *Geomech. Energy Environ.* **2022**, *32*, 100282. [CrossRef]
27. Feng, R.; Mejer Hansen, T.; Grana, D.; Balling, N. An Unsupervised Deep-Learning Method for Porosity Estimation Based on Poststack Seismic Data. *Geophysics* **2020**, *85*, M97–M105. [CrossRef]
28. Wang, M.; Zhang, X.; Wang, H.; Hui, G.; Chen, S. Integrating Geological Model via A Multimodal Machine Learning Approach in Shale Gas Production Forecast. *Gas Sci. Eng.* **2025**, *139*, 205617. [CrossRef]
29. Gamal, H.; Elkatatny, S. Prediction Model Based on an Artificial Neural Network for Rock Porosity. *Arab. J. Sci. Eng.* **2022**, *47*, 11211–11221. [CrossRef]
30. Luo, Y.; Huang, H.; Jakobsen, M.; Yang, Y.; Zhang, J.; Cai, Y. Prediction of Porosity and Gas Saturation for Deep-Buried Sandstone Reservoirs from Seismic Data Using an Improved Rock-Physics Model. *Acta Geophys.* **2019**, *67*, 557–575. [CrossRef]
31. Das, V.; Mukerji, T. Petrophysical Properties Prediction from Prestack Seismic Data Using Convolutional Neural Networks. *Geophysics* **2020**, *85*, N41–N55. [CrossRef]
32. Zhou, L.; Liao, J.; Li, J.; Chen, X.; Yang, T.; Hursthouse, A. Bayesian Time-Lapse Difference Inversion Based on the Exact Zoeppritz Equations with Blockiness Constraint. *J. Environ. Eng. Geophys.* **2020**, *25*, 89–100. [CrossRef]
33. Song, B.; Li, X.-Y.; Ding, P.; Chen, S.; Cai, J. Direct Pre-Stack Inversion of Elastic Modulus Using the Exact Zoeppritz Equation and the Application in Shale Reservoir. *Front. Earth Sci.* **2023**, *11*, 1107068. [CrossRef]

Disclaimer/Publisher's Note: The statements, opinions and data contained in all publications are solely those of the individual author(s) and contributor(s) and not of MDPI and/or the editor(s). MDPI and/or the editor(s) disclaim responsibility for any injury to people or property resulting from any ideas, methods, instructions or products referred to in the content.